DOI: https://doi.org/10.68732/0d78cde5fa8a271c

ISBN: 978-9989-2053-6-1

Analysis of Underground Roadway Stability under Geomechanical Parameters Uncertainty using RS2 Finite Element Modelling

P. Małkowski & M. Kulula
AGH Universityof Krakow, Krakow, Poland
kulula@agh.edu.pl
0000-0003-0870-438X & 0009-0008-0843-7174

Abstract

Underground roadway stability is still often assessed using a single deterministic set of rock mass inputs, which can mask the influence of natural variability in stiffness and strength. This study quantifies the effect of uncertainty in Young's modulus (E) and uniaxial compressive strength (UCS) on roadway performance using RS2 finite-element modelling. Laboratory testing of core specimens from an underground mine provided E and UCS datasets for three lithological units: claystones, siltstones, and sandstones, which were used to define input distributions. UCS was modelled as normally distributed for all lithologies, while E was normal for claystone and siltstone and lognormal for sandstone to reflect observed skewness and non-negativity.

Three complementary scenarios were analysed: (1) a deterministic Base case using laboratory mean E and UCS, (2) an ensemble mean response (μ) from 200 Latin Hypercube realisations per lithology, and (3) a statistical condition ($\mu-0.5\sigma$) reported by RS2 Interpret. Outputs focused on crown vertical displacement and roof strength factor (SF), extracted along a standardised offset query line to ensure consistent comparisons.

Results show that uncertainty effects concentrate in the weakest unit: the claystone-dominated lithology governs convergence demand and stability margin, with crown convergence reaching 28.6 mm and SF_{min} dropping to 0.96 under $\mu-0.5\sigma$. Siltstone and sandstone exhibit lower convergence and generally higher SF, providing consistency checks. Combining μ and $\mu-0.5\sigma$ offers a practical screening basis for separating expected performance from a less favourable statistical condition in variable ground.

Keywords

Underground roadway stability, Geomechanical uncertainty, Latin Hypercube sampling, RS2 modelling, Probabilistic analysis.

1 Introduction

The inherent variability of rock mass parameters creates significant challenges for decision-making in geotechnical engineering (Phoon et al. 2022). This study evaluates roadway stability using three complementary simulation scenarios that progressively move from a deterministic benchmark toward a probabilistic interpretation. The analysis investigates how different deterministic and probabilistic interpretations of laboratory-derived E and UCS affect predicted roadway response while all other parameters are held constant. The three scenarios comprised: (1) a deterministic Base case, (2) an ensemble mean response (μ) derived from Latin Hypercube realisations, and (3) a statistical condition ($\mu - 0.5\sigma$) extracted in RS2 Interpret.

The Base scenario represented the conventional deterministic approach: the use of the laboratory-derived mean values of *UCS* and Young's modulus (*E*) for each lithological unit. Its role is to provide a reference point for interpreting how much the predicted response changes once variability is acknowledged, and to mirror typical design practice where "best-estimate" properties are adopted (Phoon & Kulhawy 1999; Baecher 2003).

In the second scenario, μ represents the ensemble mean response obtained from 200 Latin Hypercube realisations for each rock type. This scenario is most useful for serviceability-type interpretation because it represents the expected model response while filtering out the influence of low-probability but high-consequence combinations within the input space (Zhao et al. 2021).

The third scenario corresponds to the statistical condition ($\mu - 0.5\sigma$) available in RS2 Interpret after the 200 Latin Hypercube realisations were completed. In this study, it is used as a practical lower-bound response indicator for comparing crown displacement and strength factor against the deterministic Base case and the ensemble mean response. In weak or variable ground, such a condition is useful because it highlights how stability margins change when the response shifts away from the central tendency toward a less favourable part of the probabilistic output range (Phoon & Kulhawy 1999; Baecher 2003; Do et al. 2022).

While probabilistic approaches have been applied to tunnel stability, fewer studies examine how parameter uncertainty derived directly from laboratory datasets propagates into numerical roadway stability predictions using practical sampling methods such as Latin Hypercube sampling. Małkowski et al. (2021) showed that the statistical processing of geomechanical input data had a substantial effect on numerical modelling results. Recent reliability analyses of deep tunnels also show that variability in rock mass properties can noticeably change predicted stability, even when deterministic results appear acceptable (Kumar et al. 2024). In this study, UCS and Young's modulus (E) were obtained from laboratory uniaxial compression tests of cylindrical specimens from three lithological units (claystones, siltstones, sandstones), providing the datasets used to define the input distributions and summary statistics. These parameters were then used to populate the three modelling scenarios described above, enabling consistent comparison of roadway stability response across rock types.

2 Geomechanical Input Characterisation

Uniaxial compressive strength (UCS) and Young's modulus (E) were determined from laboratory testing of drill core specimens obtained from an underground mine in Poland, following ISRM suggested methods (Ulusay and Hudson 2007). Core specimens had a nominal diameter of approximately 47 mm and height-to-diameter ratio of 2.5. Load rate was 0.5–1.0 MPa/s. All tests were performed under dry conditions at room temperature. Axial strain was derived from machine displacement measurements. Young's modulus was evaluated as the average modulus, calculated from the linear portion of the stress–axial strain curve. The laboratory dataset comprised 50 claystones, 79 siltstones, and 42 sandstones.

2.1 Young's modulus (*E*) distribution

Claystones and siltstones were represented by normal distributions, whereas sandstones were represented by a lognormal distribution to preserve non-negativity and accommodate observed right-skewness (Table 1).

Table 1. Statistics and probability distributions for Young's modulus, E, used as input into RS2.

Rock type	Number of Samples	Distribution	E mean [GPa]	SD [GPa]	E min [GPa]	E max [GPa]
Claystone	50	Normal	7.64	2.32	1.97	12.10
Siltstone	79	Normal	11.97	1.53	8.17	15.56
Sandstone	42	Lognormal	16.25	2.62	12.07	26.78

2.2 UCS Distribution

Table 2 shows normal distribution modelling for all three rock types. The adopted distributions capture the observed increase in strength level from claystone to sandstones, while preserving comparable scatter across datasets. The paired E–UCS samples define the probabilistic input space used in subsequent RS2 simulations for output statistics of crown displacement and strength factor.

Table 2. Statistics and probability distributions for UCS, used as input into RS2.

Rock type	Number of Samples	Distribution	UCS mean [MPa]	SD [MPa]	UCS min [MPa]	UCS max [MPa]
Claystone	50	Normal	45.07	15.91	11.52	71.37
Siltstone	79	Normal	72.57	14.06	42.80	102.78
Sandstone	42	Normal	106.56	15.30	79.07	139.72

3 Numerical model

Numerical analyses were carried out using the finite element software RS2 (version 11.027) under plane strain conditions. The model represents a horseshoe-shaped underground roadway with a width of 6m and a height of 4m, excavated in a homogeneous rock mass per analysis (each lithology modelled separately). The model size was ca. 60 m ×90 m. All model boundaries were fixed ($u_x = 0$, $u_y = 0$) at sufficient distance from the excavation to minimise boundary influence. Initial in-situ stresses were applied prior to excavation, corresponding to a depth of approximately 700 m (σ_v = 17.5 MPa), in lithological state of stress $\sigma_v = \sigma_H = \sigma_h$.

Rock mass behaviour was modelled using the generalised Hoek–Brown failure criterion with residual strength included ($\sigma_{cr} = 0.1\ \sigma_c$). The adopted RMR values were 40 for claystone, 50 for siltstone, and 60 for sandstone. Elastic–plastic analyses were performed using a staged excavation approach, consisting of an initial intact rock stage followed by instantaneous excavation of the roadway. No support elements were included at this stage, as the analyses were intended to first evaluate inherent ground stability. A graded finite element mesh with triangular elements was adopted. Mesh density was increased near the roadway boundary.

For probabilistic analyses, a sample size of 200 Latin Hypercube realisations was adopted in RS2 to obtain stable statistical estimates while maintaining computational efficiency (Fenton & Griffiths 2008). Only Young's modulus (E) and uniaxial compressive strength (UCS) were treated as random variables, assumed to be statistically independent, while all other parameters were held constant. Model outputs focused on crown vertical displacement and strength factor distributions. For interpretation, RS2 summary outputs were used to extract the Base file values, the ensemble mean response (μ), and the statistical condition ($\mu - 0.5\sigma$) for each lithology. Roof stability was assessed using Strength Factor (SF) extracted along a query line parallel to the crown/shoulder boundary and offset 0.4–1.4m into the rock mass to minimise boundary artefacts and standardise extraction across scenarios (Rocscience 2026).

4 Results and Discussion

4.1 Vertical Displacement

Vertical displacement provides a direct measure of roadway convergence demand and is therefore used here as the primary serviceability indicator (Fig. 1). In the claystone rock mass, the base case yields a peak displacement of 27.0 mm, with deformation concentrated around the excavation boundary (Fig. 1a). The probabilistic ensemble mean shows a similar pattern with a slightly lower peak of 26.9 mm (Fig. 1b), indicating that sampling of UCS–E variability only marginally changes the expected deformation relative to the deterministic benchmark. In contrast, the $\mu - 0.5\sigma$ scenario

amplifies deformation, with peak displacement rising to 28.6 mm, about 5.93% above the base case (Fig. 1c). For the sandstone rock mass, deformation remains much smaller across all scenarios, with peak displacement of 7.81 mm in the base case, 7.89 mm for the ensemble mean, and 8.20 mm under $\mu-0.5\sigma$ (Fig. 1d–f). This indicates that, unlike claystone, sandstone response is comparatively insensitive to the imposed UCS–E variability, with only a modest increase of 4.99% in the adverse case relative to the base case. Overall, the comparison shows that less favourable probabilistic response conditions increase deformation demand mainly in the weaker claystone, whereas the stronger sandstone provides a comparatively stable serviceability response under the same stress conditions.

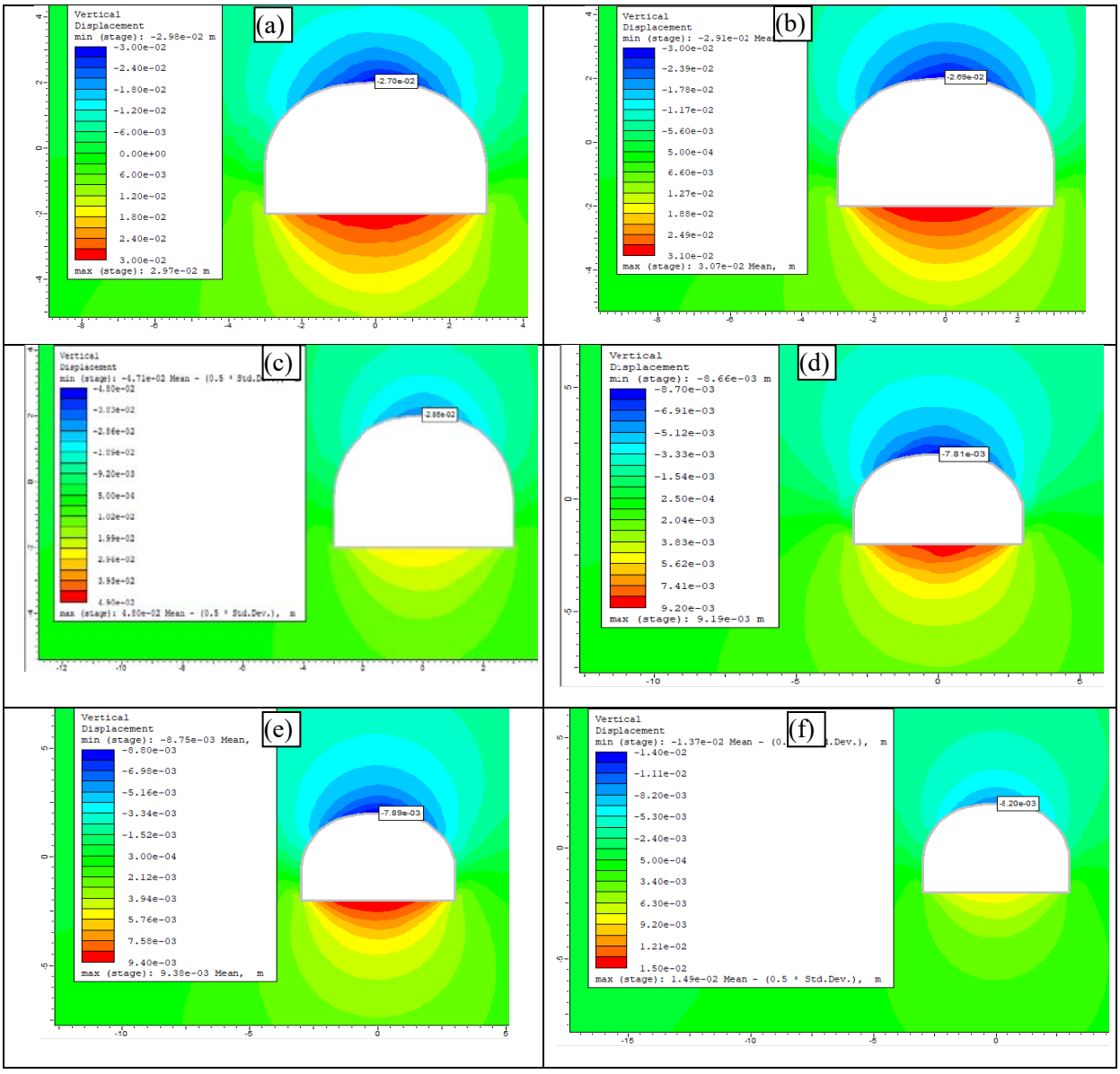


Fig. 1 Vertical displacement contours: for the claystone rock mass(a) base case, (b) ensemble mean, (c) μ−0.5σ, for the sandstone rock mass (d) base case, (e) ensemble mean, (f) μ−0.5σ.

4.2 Strength Factor

For the claystone rock mass, the strength factor (SF) response indicates a near-limit state along the offset roof query line, with scenario selection strongly influencing whether the crown is interpreted as stable or yield-prone (Fig. 2a–c). In the base case, the crown query line spans 1.00–1.25, with a local minimum of 1.00, implying that parts of the roof/shoulder region are at the threshold of yielding (Fig. 2a). The ensemble mean shifts the full query line above unity (1.02–1.38), reducing the apparent risk relative to the deterministic benchmark (Fig. 2b). In contrast, the μ−0.5σ case compresses the crown response tightly around unity (0.96–1.07) and produces three locations with SF < 1.0, indicating an enlarged yield-prone roof zone under the $\mu-0.5\sigma$ statistical condition (Fig. 2c).

For the sandstone rock mass, the SF field is more regular and symmetric, but the crown response also remains close to the SF = 1 threshold (Fig. 2d–f). The minimum SF increases from 1.00 in the base

case to 1.01 for the ensemble mean, before dropping to 0.98 under $\mu-0.5\sigma$. Overall, both lithologies remain sensitive to scenario definition at the crown, with the probabilistic mean slightly increasing the apparent stability margin and the $\mu-0.5\sigma$ case reducing it below 1. Unlike the displacement results, the SF response shows a weaker lithological contrast, indicating that local crown stability remains scenario-sensitive in both rock masses.

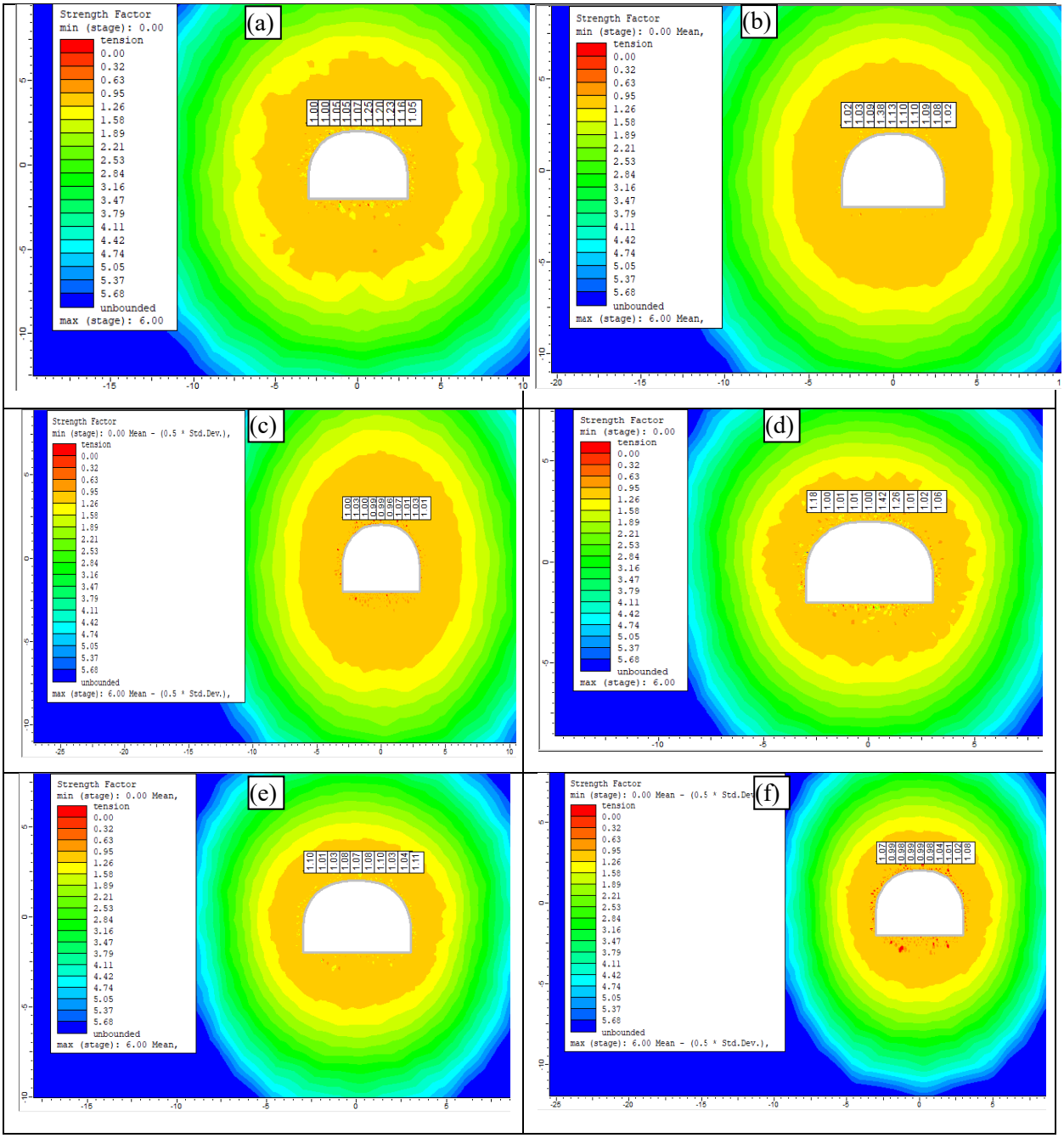


Fig. 2 Strength factor (*SF*) contours for: the claystone rock mass (a) base case, (b) ensemble mean, (c) μ−0.5σ,the sandstone rock mass (d) base case, (e) ensemble mean, (f) μ−0.5σ.

4.3 Cross-lithology analysis

Consistent with reliability-based rock engineering practice (Einstein et al. 2010), the cross-lithology results show that claystone governs both convergence demand and crown stability margin, whereas the stronger rock masses show lower $|u_y|$ and generally higher SF values (Table 3). Siltstone occupies an intermediate position between claystone and sandstone, with crown displacement of 14.30 – 17.90 mm and SFmin ≥1.00 in all scenarios, indicating that uncertainty mainly reduces reserve capacity rather than triggering yield. From a design perspective, μ represents expected serviceability, whereas $\mu-0.5\sigma$ provides a practical lower-bound check on the model response; where it gives SF < 1.00 at the roof or a marked increase in crown displacement, preliminary support decisions should be guided by that less favourable condition unless support and excavation sequence are explicitly modelled (Bjureland 2020; Hoek 2023).

Table 3. Crown displacement and strength factor at the roof for each lithology and scenario.

Rock type	Scenario	$\|u_\gamma\|$ at crown (mm)	SFmin at crown	$\Delta\|u_\gamma\|$ vs Base (%)	ΔSFmin vs Base (%)
Claystone	Base	27.0	1.00	0.00	0.00
	μ	26.9	1.02	-0.37	2.00
	$\mu - 0.5\sigma$	28.6	0.96	5.93	-4.00
Siltstone	Base	15.3	1.00	0.00	0.00
	μ	14.3	1.01	-6.54	1.00
	$\mu - 0.5\sigma$	17.9	1.00	16.99	0.00
Sandstone	Base	7.8	1.00	0.00	0.00
	μ	7.9	1.01	1.02	1.00
	$\mu - 0.5\sigma$	8.2	0.98	4.99	-2.04

5 Conclusion

Probabilistic RS2 simulations using Latin Hypercube sampling show that uncertainty in Young's modulus and UCS affects roadway performance, with the response controlled by the weakest lithology. The claystone rock mass governs behaviour: under the $\mu-0.5\sigma$ statistical condition, crown displacement increases to 28.6 mm and the stability margin reduces to SF_{min} = 0.96, showing that a less favourable probabilistic response can move the system closer to yield. Siltstone and sandstone show lower displacement demand overall, while siltstone maintains $SF_{min} \geq 1.00$ across scenarios. Taken together, μ and $\mu-0.5\sigma$ provide a practical basis for preliminary design screening by separating expected performance from a less favourable statistical condition in variable ground.

References

Baecher GB (2003) Reliability and statistics in geotechnical engineering. John Wiley & Sons, Chichester

Bjureland W (2020) Reliability-based design of rock tunnel support. KTH Royal Institute of Technology, Stockholm.

Do DP, Guo X, Dias D (2022) Probabilistic Stability Analysis of Deep Rock Tunnel Excavated by Mechanized Tunneling Considering Anisotropic Initial Stresses. Applied Sciences 12:7479. https://doi.org/10.3390/app12157479.

Einstein HH, Sousa RL, Karam K, et al (2010) Rock slopes from mechanics to decision making. In: Rock Mechanics in Civil and Environmental Engineering. CRC Press, Lausanne (Switzerland), pp 3-13.

Fenton GA, Griffiths DV (2008) Risk Assessment in Geotechnical Engineering. In: Risk Assessment in Geotechnical Engineering. John Wiley & Sons, Ltd, pp i–xvii.

Hoek E (2023) Practical Rock Engineering. Rocscience, North Vancouver, British Columbia, Canada.

Kumar A, Maurya S, Tiwari G (2024) Reliability analysis of deep tunnels in spatially varying brittle rocks using interval and random field modelling. International Journal of Rock Mechanics and Mining Sciences 181:105836. https://doi.org/10.1016/j.ijrmms.2024.105836.

Małkowski P, Niedbalski Z, Balarabe T (2021) A statistical analysis of geomechanical data and its effect on rock mass numerical modeling: a case study. International Journal of Coal Science and Technology, 8(2), pp. 312–323, https://doi.org/10.1007/s40789-020-00369-2.

Phoon K-K, Cao Z-J, Ji J, et al (2022) Geotechnical uncertainty, modeling, and decision making. Soils and Foundations 62:101189, https://doi.org/10.1016/j.sandf.2022.101189.

Phoon K-K, Kulhawy FH (1999) Characterization of geotechnical variability. Canadian Geotechnical Journal 36:612–624.

Rocscience (2026) RS2 Documentation_Query Boundary. https://www.rocscience.com/help/rs2/documentation/rs2-interpret/material-queries/query-boundary?utm_source=chatgpt.com,accessed 9 Feb 2026.

Ulusay R, Hudson JA (2007) The Complete ISRM Suggested Methods for Rock Characterisation, Testing and Monitoring 1974-2006. ISRM Turkish National Group.

Zhang H, Luo F, Yang S, Wu Y (2023) Probabilistic analysis of crown settlement in high-speed railway tunnel constructed by sequential excavation method considering soil spatial variability. Tunnelling and underground space technology 140:105342,https://doi.org/10.1016/j.tust.2023.105342.

Zhao H, Li S, Zhu C (2021) Uncertainty analysis of rock tunnel based on fractional moment and dimensional reduction method. International Journal of Rock Mechanics and Mining Sciences 139:104656, https://doi.org/10.1016/j.ijrmms.2021.104656.